

Supplemental Data

Supplemental Results

*Premature nuclear division observed in HU or MMS treated *mec1* cells could be rescued by depletion of *Ndd1**

It is well known through several studies that *mec1* mutants cannot prevent premature spindle elongation and nuclear division upon HU or MMS treatment due to lack of active checkpoints (1). Since it was shown that an active Mec1 checkpoint will inhibit the transcription of G2/M-specific genes by preventing Ndd1 recruitment, the abnormal behavior of *mec1* cells might be caused by inappropriate and prematurely high expression of G2/M specific gene products. We therefore examined whether down-regulation of G2/M transcription by Ndd1 depletion in genotoxically stressed *mec1* mutants could suppress their abnormal spindle phenotype. Normally, in the absence of Ndd1, the inability of cells to undergo cytokinesis was the main distinct phenotype but cells still produced elongated spindles and divided their nuclei, albeit with slower kinetics when compared to the cells expressing Ndd1 (Fig. S6A & B). To test whether precocious spindle elongation and nuclear division observed in genotoxically stressed *mec1* mutant could be suppressed with Ndd1 depletion, we synchronized SKY299 cells in G1 in YEP-raf-gal, released half of the culture into YEP-raf-gal + HU or MMS and the remaining half into YEP-glucose + HU or MMS. As controls, *sml1* and *sml1 mec1* strains both having the wild-type copy of *NDD1* at its genomic locus were also synchronized in G1 and released into YEP-glucose. We followed kinetics of spindle elongation and nuclear division. Indeed, premature spindle elongation and nuclear division was observed in both MMS and HU challenged *sml1 mec1* strains expressing *NDD1* but not in the *sml1* strain (Fig. S6C & D; Fig. S7A - D). Depletion of *NDD1* significantly reduced the premature spindle elongation and nuclear division observed in MMS or HU challenged *sml1 mec1* cells. Conversely, over-expression of *NDD1* facilitates faster nuclear division rates during HU treatment in *sml1 mec1*

cells than control strains (Fig. S6D, Fig. S7C & D). Furthermore, Ndd1 over expression increases the sensitivity of *mecl* mutant towards MMS treatment (Fig. S7E).

Supplemental Figure Legends

FIG S1. Genotoxic stress down-regulate G2/M transcription by inhibiting the

recruitment of Ndd1. HU treatment prevents full activation of G2/M specific transcription.

(A) Wild-type strain expressing *NDD1-HA* (pHEL06) on a centromeric plasmid was synchronized in G1 and released into YEPD +/- HU. *SWI5* transcription was analyzed by northern blot analysis from the samples isolated at indicated time points. (B) Inhibition of G2/M transcription by MMS treatment is dosage dependent. Wild-type strain (SKY101) was synchronized in G1 and released into YEPD +/- 0.0075%MMS or 0.015%MMS. *CLB2* transcription was analyzed using northern blot analysis from the samples isolated at indicated time points. (C) – (E) Ndd1 recruitment to G2/M specific gene promoters is inhibited by genotoxic stress. A *NDD1-HA* (MK155) strain was synchronized in G1 and released into YEPD +/- HU or MMS. Ndd1-HA ChIP followed by q-PCR analysis targeted to *CDC5* (C), *CDC20* (D) and *ASE1* (E) promoters was performed from the samples isolated at indicated time points. (F) Ndd1 binding to *CLB2* promoter and the transcription of *CLB2* gene are inhibited upon activation of G2/M checkpoint in *cdc13-1* cells grown at non-permissive temperature. *NDD1-HA* (SKY260) and *cdc13-1 NDD1-HA* (SKY305) strains were synchronized in G1 and released into YEPD at 37°C. Ndd1-HA ChIP and *CLB2* northern blot were performed from samples isolated at indicated time points. In all of the figures, error bars indicate standard deviation in at least two independent experiments.

FIG S2. Transcription of *NDD1* is down-regulated during genotoxic stress. A) *NDD1*

mRNA levels were detected in the samples mentioned in Fig.1A by northern blot analysis.

Error bars indicate standard deviation in two independent experiments.

FIG S3. HU treatment affects the recruitment of Fkh2 to G2/M promoters, but do not influence Sin3 binding. (A) *SIN3-HA* (MK257) strain was synchronized in G1 and released into YEPD +/- HU. Sin3 recruitment to *CLB2* promoter was examined by ChIP followed with q-PCR analysis. Error bars indicate standard deviation in three independent experiments. (B) *FKH2-HA* (JV717) strain was synchronized in G1 followed by release into YEPD +/- HU. Fkh2 recruitment to *SWI5* promoter was examined by ChIP followed with q-PCR analysis. (C) *NDD1* transcription control for FIG 2B. *NDD1* mRNA levels were barely detectable when cells expressing the sole copy of *NDD1* under *GAL1-10* promoter were grown in YEP-Glucose. A *GAL 1-10* promoter regulated *NDD1* strain expressing *FKH2-MYC* (SKY270) was synchronized in G1 and released into YEP-raf/gal (Ndd1) or YEP-glucose (ndd1). *NDD1* mRNA was detected by northern blot from samples isolated at indicated time points. * indicates non-specific band.

FIG S4. Mec1-Rad53 dependent and independent signals regulate G2/M transcription upon genotoxic stress. A) Cell cycle analysis of the samples from Fig. 3 & 4 by FACS.

FIG S5. Multiple genotoxic stress induced phosphorylations inhibit the function of Ndd1. (A) DNA content analysis of Ndd1-CD-10A samples described in Fig. 7 D & E. (B) Ndd1-CD-10A mutant could partially bypass MMS induced suppression of G2/M specific genes. Northern blot analysis to detect *CLB2* mRNA was performed from the samples described in Fig. 7D. (C) & (D) Mutating additional genotoxic stress induced phosphosites on Ndd1 do not show any additive effect on Ndd1 recruitment to *CLB2* promoter in MMS treated cells. (C) Model depicting mutations introduced in *NDD1-CD-11A*. (D) JV323 cells transformed with *NDD1-CD-11A* were synchronized in G1 and release into YEPD +/- MMS. Ndd1 recruitment to *CLB2* promoter was examined by ChIP followed with q-PCR analysis.

FIG S6. Depletion of Ndd1 significantly reduces premature nuclear division observed in HU or MMS treated *mec1* cells. (A) & (B) Under normal conditions, depletion of Ndd1 delays spindle elongation and nuclear division. (A) *sml1 mec1* strain in which the only copy of *NDD1* is under the control of *GAL1-10* promoter (SKY299) was synchronized in G1 in YEP-raf-gal media. Subsequently half of the culture was released in YEP-raf-gal and the remaining half in YEP-glucose to switch off *NDD1* expression. Samples collected at the indicated time points were scored for budding index, spindle elongation and nuclear division. (B) After 180', cells grown in glucose were fixed and processed to visualize spindles and nucleus. (C) & (D) Depletion of Ndd1 in *mec1* strain significantly reduces premature nuclear division upon MMS or HU treatment. SKY299 cells were synchronized in G1 and released into YEP-raf-gal +/- MMS (C), YEP-raf-gal +/- HU (D), YEPD +/- MMS (C) and YEPD +/- HU (D). As controls, *sml1* (SKY323), *sml1 mec1* (SKY322) strains were synchronized in G1 and released into YEPD +/- MMS (C) or YEPD +/- HU (D). Samples collected at the indicated time points were scored for nuclear division.

FIG S5. Depletion of Ndd1 significantly reduces premature spindle elongation observed in HU or MMS treated *mec1* cells. (A) - (D) SKY299 cells were synchronized in G1 and released into YEP-Raf-Gal +/- MMS (A & B), YEP-Raf-Gal +/- HU (C & D), YEPD +/- MMS (A & B) and YEPD +/- HU (C & D). As controls, *sml1* (SKY323), *sml1 mec1* (SKY322) strains were synchronized in G1 and released into YEPD +/- MMS (A & B) or YEPD +/- HU (C & D). Samples collected at the indicated time points were scored for spindle elongation (spindle length $\geq 2\mu\text{M}$) (A & C) and anaphase spindles (spindle length $\geq 4\mu\text{M}$) (B & D). (E) Ndd1 over expression increases the sensitivity of *mec1* mutant to MMS treatment. A *mec1* mutant expressing *NDD1* under the control of *GAL 1-10* promoter (JV751) or from its genomic locus (JV753) was synchronized in G1 in YEP-raf-gal. Subsequently, half of the cultures were released into YEP-raf-gal MMS and the remaining half into YEP-glucose

MMS. At the time points indicated, the number of colony-forming units (CFU) in each condition was determined by plating 10^4 serial diluted cells on YEP-raf-gal medium and counting the number of colonies after 3 days of growth at 30°C. % viability of each culture was expressed as ((CFU at that time point after treatment/CFU after 0' treatment)*100). As a control, *MEC1* strain expressing *NDD1* under the control of *GAL 1-10* promoter was used.

Supplemental Table legends

Table S1. Complete list of both unphosphorylated and phosphorylated Ndd1 peptides detected in various MS runs. Ndd1 peptides identified from all experiments with phosphorylation site assignment. *sml1* (SKY174), *sml1 rad53* (SKY325) and *sml1 mec1* (SKY170) strains expressing Ndd1-HTB-eaq were synchronized in G1 and released into YEPD +/- HU or MMS. Mass spectrometry analysis was performed with Ndd1-HTBeaq purified from these conditions. Complete list of phosphorylated and un-phosphorylated peptides identified is provided along with the corresponding site probabilities and additional raw data.

Table S2. List of strains and plasmids used in supplemental results

Supplemental Experimental Procedures

FACS and Fluorescence microscopy

For FACS analysis, 1ml of culture was spun down at 14k rpm for 30''. Cells were fixed in 70% ethanol and digested with RNase in 50mM Tris pH7.5 overnight at 37°C. Later, RNase was washed off and cells were suspended in 200mM Tris PH 7.5, 211mM NaCl, and 78mM MgCl₂ buffer with 0,05mg/ml propidium iodide and sonicated gently. 20microlitres of this cell suspension was diluted in 1ml of 50mM Tris pH7.5 and used for FACS analysis using BD FACScalibur. 3D overlay graphs were generated with WinMDI 2.5 software. For fluorescence microscope analysis, 1ml of culture was spun down at 14k rpm for 30''. Cells

were fixed in 70% ethanol and resuspended in 30mM Sodium citrate, 300mM NaCl buffer. Nuclear staining was done by incubating the cells in 1XPBS buffer with Hoechst 33342 (Molecular Probes). Cells were washed twice with 1X PBS buffer to get rid of unbound dye and directly used for fluorescence microscopy studies using personal Delta Vision Epifluorescence microscope from Applied Precision Inc. Nuclear division and spindle elongation was quantified manually using ImageJ software (2). At least 50 cells were counted for each time point.

LC-MS/MS analysis

Beads were washed five times with ammonium bicarbonate buffer (50mM ABC). Disulfide bonds were reduced with dithiothreitol (1:20 of the estimated amount of protein) and Cys-residues were subsequently alkylated with iodoacetamide (IAA) (1:4 of the estimated amount of protein). DTT (1:20 of the estimated amount of protein) was added to consume excess IAA and proteins were digested with trypsin (recombinant, proteomics grade, Roche; 1:20 of the estimated amount of protein) at 37°C overnight. Digests were stopped by addition of trifluoroacetic acid (TFA) to approx. pH 2.

Digests were separated on an UltiMate 3000 HPLC system (Thermo Fisher Scientific). Peptides were loaded on a trapping column (PepMap C18, 5 µm particle size, 300 µm i.d. x 5 mm, Thermo Fisher Scientific) equilibrated with 0.1% TFA and separated on an analytical column (PepMap C18, 3 µm, 75 µm i.d. x 150 mm, Thermo Fisher Scientific) applying a 60 minutes linear gradient from 2.5% up to 40% acetonitrile (ACN) with 0.1% formic acid followed by a washing step with 80% ACN and 10% TFE (trifluoroethanol). The HPLC was directly coupled to an LTQ-Orbitrap Velos mass spectrometer (Thermo Fisher Scientific) via a nanoelectrospray ionization source (Thermo Fisher Scientific). The electrospray voltage was set to 1500 V. The mass spectrometer was operated in the data-dependent mode: 1 full scan (m/z: 400-1800, resolution 60000) with lock mass enabled was followed by maximal 20

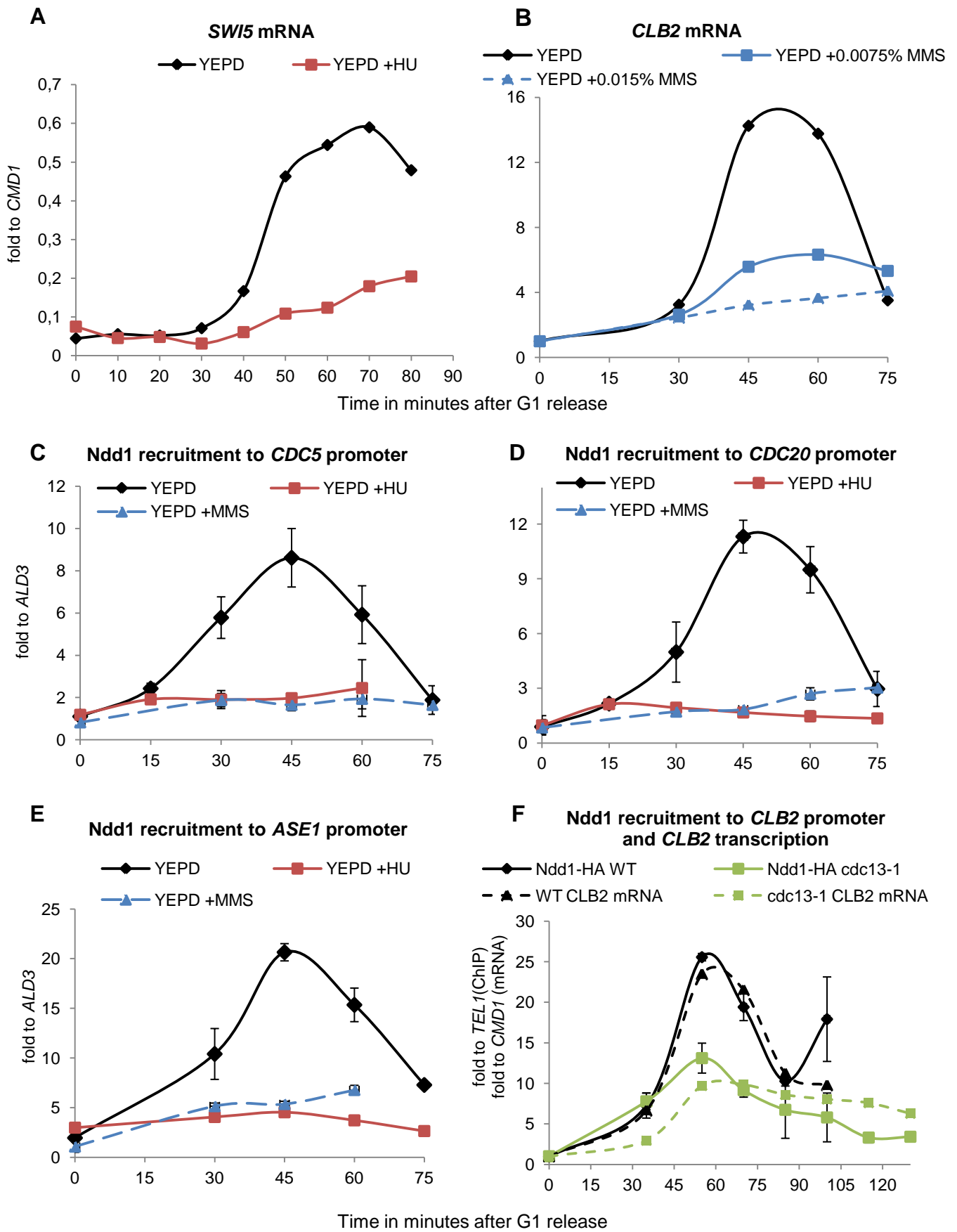
MS/MS scans. Neutral losses of 98, 49 and 32.6 in the MS2 triggered an MS3 analysis in the linear ion trap. The lock mass was set at the signal of polydimethylcyclsiloxane at m/z 445.120025. Monoisotopic precursor selection was enabled, singly charged signals were excluded from fragmentation. The collision energy was set at 35%, Q-value at 0.25 and the activation time at 10 msec. Fragmented ions were excluded from further selection for 30 s.

Peptide identification was performed using the SEQUEST algorithm in the Proteome Discoverer 1.3.0.339 software package (Thermo Fisher Scientific). Spectra were searched against the SGD database (6717 entries, 03-Feb-2011) that has been extended manually by the sequences of common contaminants. Carbamidomethylation of Cys was set as static modifications. Phosphorylation of Ser/Thr/Tyr and oxidation of Met were set as variable modifications. Protease specificity was set to tryptic allowing two missed cleavages, a peptide tolerance of 2 ppm, a fragment ions tolerance of 0.5 Da. The results were filtered at the Xcorr values to an FDR of 1% on the peptide level. The probability of phosphorylation site localization was calculated using the phosphoRS software (3) implemented into Proteome Discoverer. A phosphorylation site probability of 75% or higher was considered as confidently localized. Annotated MS/MS spectra were exported for all peptide-spectrum matches that mapped to Ndd1.

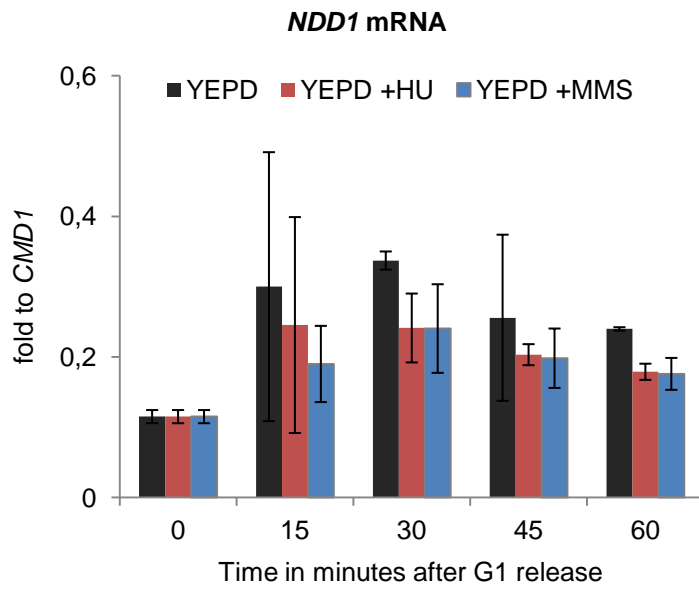
Supplementary References

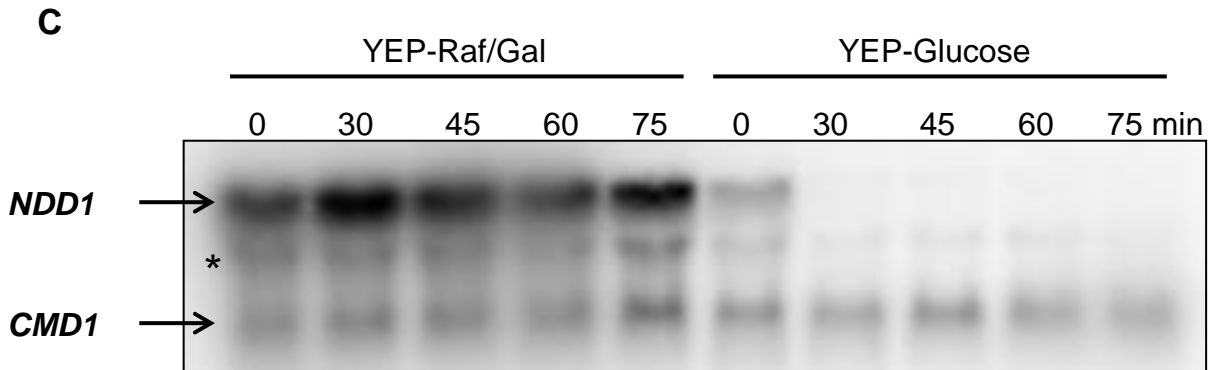
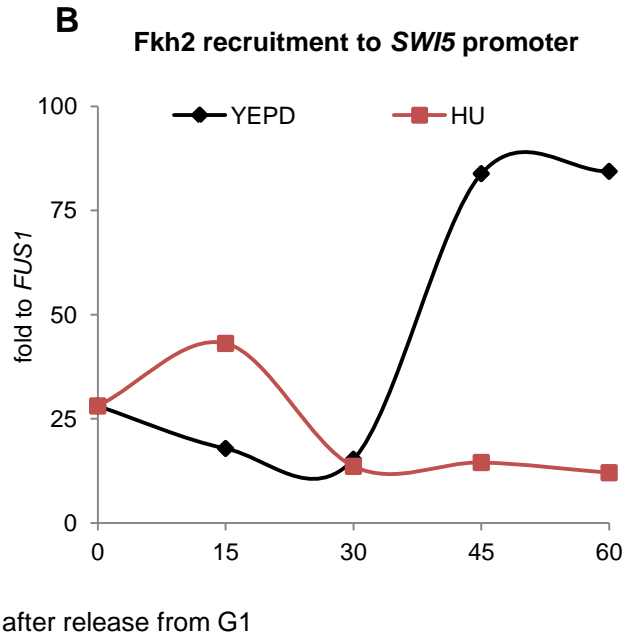
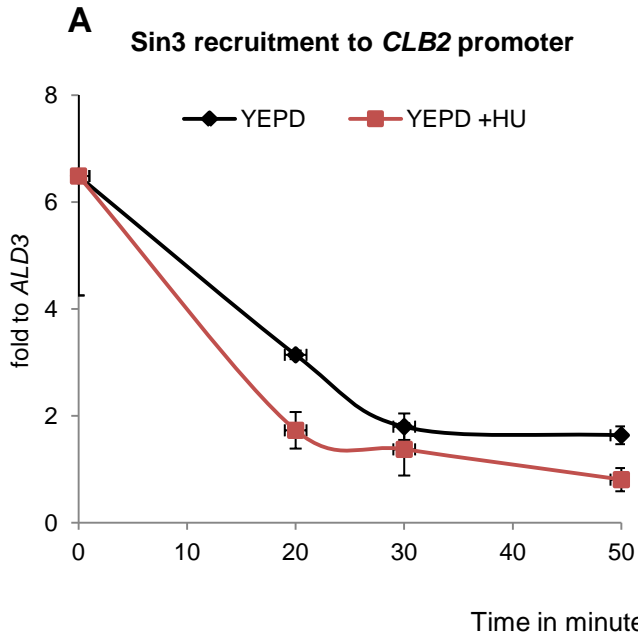
1. **Krishnan V, Nirantar S, Crasta K, Cheng AY, Surana U.** 2004. DNA replication checkpoint prevents precocious chromosome segregation by regulating spindle behavior. *Molecular cell* **16**:687-700.
2. **Schneider CA, Rasband WS, Eliceiri KW.** 2012. NIH Image to ImageJ: 25 years of image analysis. *Nat Meth* **9**:671-675.

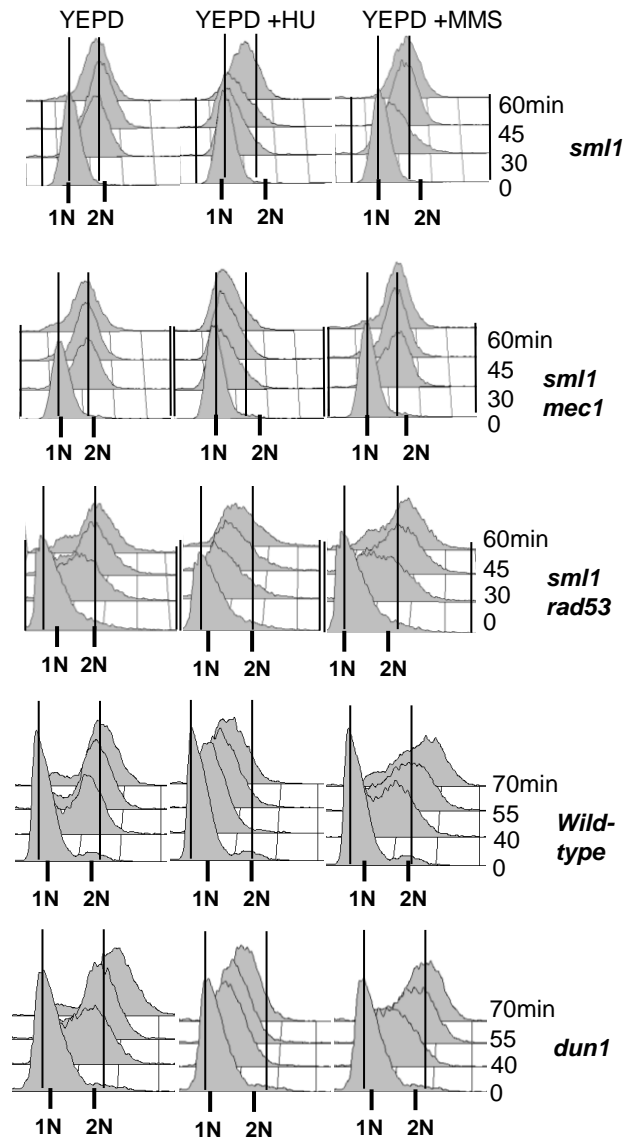
3. **Taus T, Kocher T, Pichler P, Paschke C, Schmidt A, Henrich C, Mechtler K.**
2011. Universal and Confident Phosphorylation Site Localization Using phosphoRS. *J Proteome Res* **10**:5354-5362.

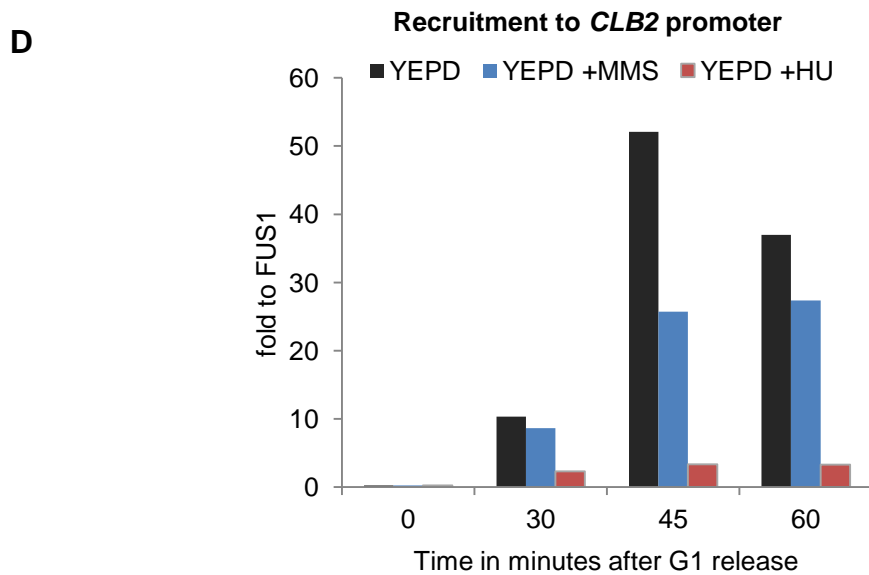
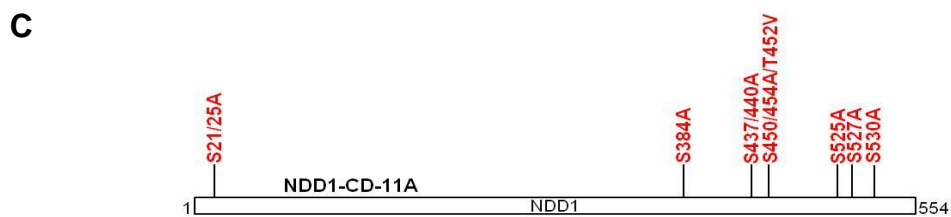
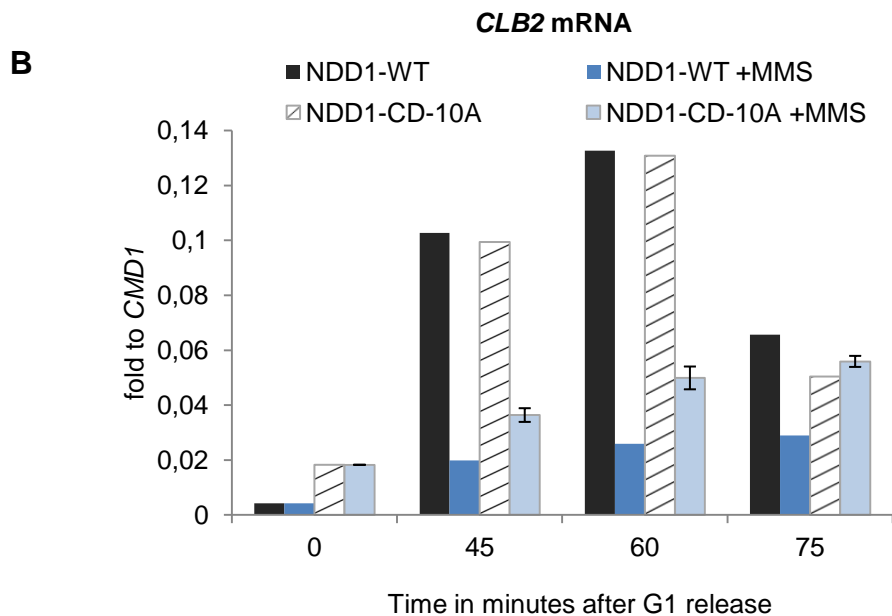
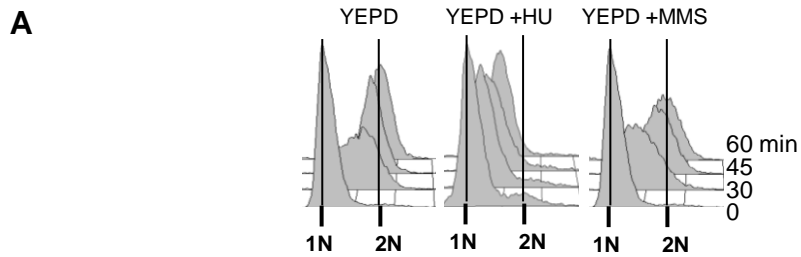


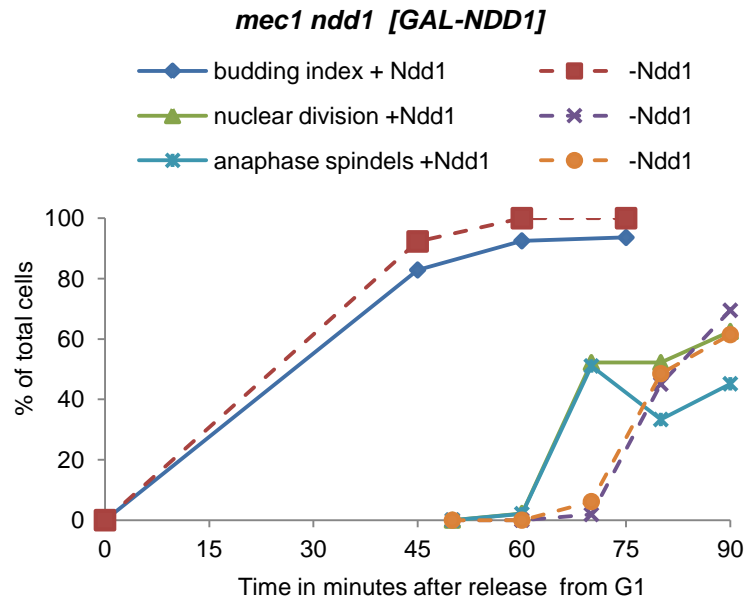
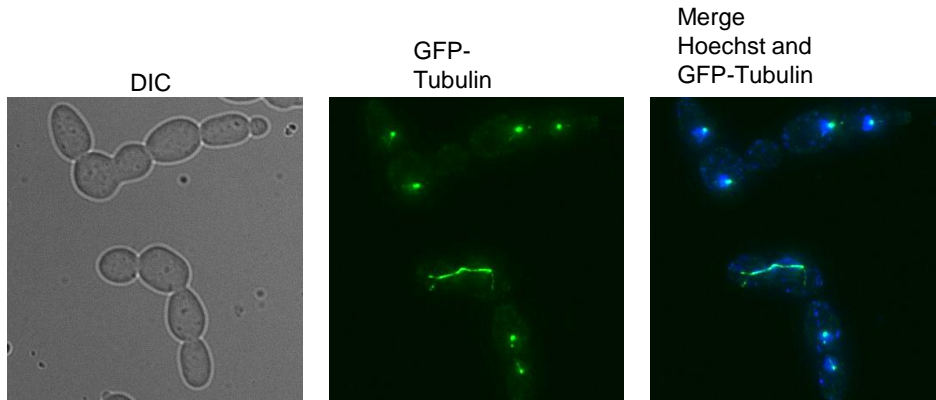
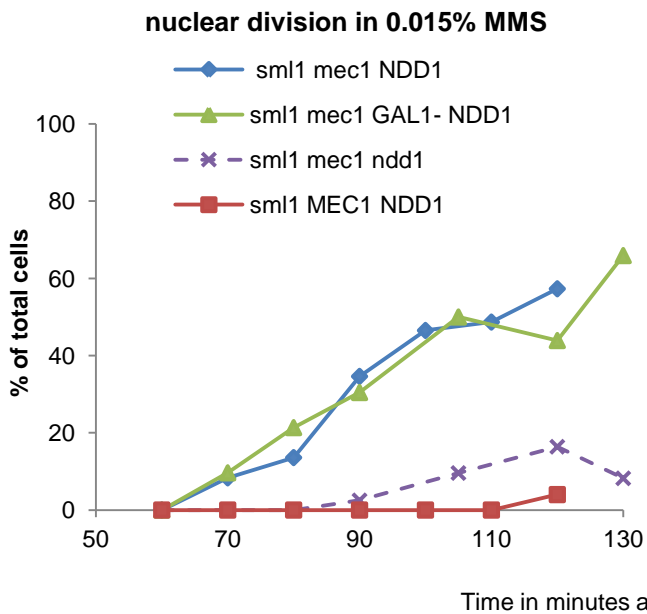
A





A



A**B****C****D**